Rare earth elements interaction with iron-organic matter colloids as a control of the REE environmental dissemination

Yasaman Tadayon, Delphine Vantelon, Julien Gigault, Aline Dia, Maxime Pattier, Lionel Dutruch, Mélanie Davranche

Journal of Colloid and Interface Science 655 (2024) 70–79

Contents lists available at ScienceDirect

Journal of Colloid And Interface Science

journal homepage: www.elsevier.com/locate/jcis

Rare earth elements interaction with iron-organic matter colloids as a control of the REE environmental dissemination

Yasaman Tadayon [a,*], Delphine Vantelon [b], Julien Gigault [c], Aline Dia [a], Maxime Pattier [a], Lionel Dutruch [a], Mélanie Davranche [a]

[a] Univ. Rennes, CNRS, Géosciences Rennes, UMR 6118, F-35000 Rennes, France
[b] Synchrotron SOLEIL, L'orme des merisiers, Saint Aubin BP48, 91192 Gif sur Yvette Cedex, France
[c] TAKUVIK CNRS/ULaval, UMI3376, Université Laval, Quebec City, QC, Canada

GRAPHICAL ABSTRACT

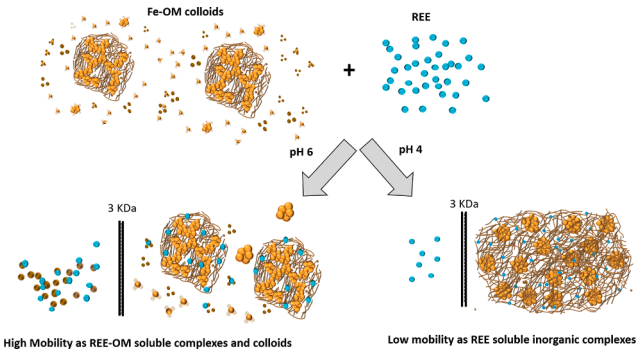

ARTICLE INFO

Keywords:
Colloids
Organic matter (OM)
Iron (Fe)
Rare earth elements (REE)
Heterogenous colloids
pH
Adsorption
Mobility
Aggregation
Fe-OM aggregates

ABSTRACT

Rare earth elements (REE) are highly sought after for advanced technology, in response concerns about their environmental impact have arisen. The mobility and transport of REEs are influenced by their binding to solid surfaces, particularly colloids. With the widespread occurrence of REEs and their potential increase due to climate change, there is growing interest in understanding colloids composed of organic matter (OM) and iron (Fe). The reactivity of these colloids depends on their structural organization and the availability of Fe phase and OM binding sites. The effect of pH on the binding and mobility of REEs in these colloids in response to structural modification of Fe-OM colloids was investigated. REEs are primarily bind to the OM component of Fe-OM colloids, and their mobility is controlled by the response of OM colloids and molecules to pH conditions. At pH 6, the solubilization of small organic colloids (<3 kDa) control the REE pattern and subsequent speciation and mobility. In contrast, at pH 4, Fe-OM colloids bind less amount of REE but aggregate to form a large network. While most REEs remain soluble, those bound to Fe-OM colloids are expected to be immobilized through settlement or trapping in soil and sediment pores.

This study supports the idea that colloids control the REE speciation and subsequent dissemination. The findings are particularly relevant for assessing the fate and ecotoxicology of REE in response to changing environmental conditions and increasing REE concentration in natural systems.

* Corresponding author.
E-mail address: yasaman.tadayon@univ-rennes1.fr (Y. Tadayon).

https://doi.org/10.1016/j.jcis.2023.10.110
Received 19 June 2023; Received in revised form 6 September 2023; Accepted 20 October 2023
Available online 30 October 2023

1. Introduction

The development of new green energy technologies is bases on 'novel' strategic chemical elements such as the rare earth elements (REE). This group of elements comprise 15 lanthanides as well as Yttrium (Y) and Scandium (Sc). They have gained significant prominence since they are extensively employed in a wide range of industrial and technological applications, primarily for energy storage purposes to reduce greenhouse gases (wind turbines, hybrid cars, etc.). The upcoming industrial revolution is predicted to be the new green energy transitions [1–3]. Rare earth elements are used in agriculture as well, and numerous reports have highlighted their absorption by plants [4]. Gadolinium (Gd), is also used in magnetic resonance imaging (MRI) as a contrast enhancer [5]. Moreover, as REE are becoming a matter of great economic interest, their significant release into the environment is expected over the next few decades. As green technologies continue to advance and find greater application in agriculture, high tech products, etc., REE are likely to be more and more extracted. Their recycling is increasingly gaining attention, however various challenges exist in technologies and methods for REE recovery [6]. Processes to extract REE from secondary sources are under development, it is not yet clear which will be profitable at scale [7] and recycling satay less profitable than extraction for some of recovery processes [8]. This increasing extrication results in the disruption of REE biogeochemical cycles. However, knowledge gaps exist regarding the substantial short and long-term release of REEs into the environment. The enduring exposure of REE can inflict harm upon animals, plants, and human health [9]. High levels of REEs have been associated with organ-specific toxicity, growth inhibition, pneumoconiosis, and nerve diseases source. Consequently, there is mounting concern about REE in recent years, leading to their consideration as emerging pollutants [10,11]. Hence, it becomes crucial to assess their sources, transportat pathways and potential health and environmental hazards.

Environmental nanoparticles are common in natural systems [12–14]. They are known to play an important role in the distribution and transportation of chemical elements. Among those nanoparticles, natural iron-organic matter (Fe-OM) aggregates are particularly important because of their abundance in natural systems such as wetlands [15–17], peatlands [18,19] and permafrost [20,21]. They are primarily produced in soil as a result of anthropogenic forcing and geochemical and physical processes such as alteration and erosion, as well as oxidation-reduction variations that occur in response to the soil water-saturation/desaturation alternation [16]. Due to global warming, involving an increase in rainfall frequency, volume, and intensity as well as permafrost thawing, the production of these nano-aggregates or colloids has tended to significantly increase in recent decades.

As recently described, inside Fe-OM aggregates, weakly crystallized Fe oxyhydroxides are embedded in an OM matrix following a fractal organisation [22–25]. Organic matter as molecules and colloids [22–24] limit the growth and crystallinity of the Fe phases [26,27]. As a result, Fe generates Fe(III) monomers, tiny oligomers, and ferrihydrite-like nanoparticles (Fh-like Nps) linked to the OM via the carboxylic (COOH) and phenolic (PhOH) sites [22,27–32]. The Fh-like Nps have fractal organization and are made of primary beads (radius 0.8 nm) that combine to generate primary aggregates (radius 4 nm), which aggregate to form secondary aggregates (radius >100 nm) embedded into larger OM aggregates (radius ~700 nm) [22,24].

Because of the high affinity of OM and Fe phases for metallic elements, REE are expected to bind to these aggregates [33–35]. Therefore, Fe-OM aggregates physical and chemical properties and stability control the metallic elements mobility through the soil and aqueous system. However, mechanisms controlling the interactions between metallic elements and Fe-OM aggregates are still unclear. For a long time, the sorption capacities of heterogeneous aggregates were assuming to follow an additive rule. However, Guénet et al. (2017) revealed that the sorption capacity of Fe-OM aggregates increases with the increasing Fe/organic carbon (OC) ratio while the specific surface area (SSA) of Fe-NPs remained constant, demonstrating that the SSA is not the sole parameter that governs the reactivity of Fe-OM aggregates. Additionally, Calcium (Ca) can significantly impact the structural organization of the Fe-OM aggregates [22]. High Ca concentrations produce the Fe-OM aggregates structural modifications, transitioning from a colloidal state to a non-colloidal micrometric Ca-branched OM network in which Fh-like Nps remained embedded. This drastic modification is mostly caused by the binding of Ca to the OM COOH sites. According to Beauvois et al. (2020) and Davis and Edwards (2017), under these conditions, two antagonistic effects are anticipated when the interactions between Fe and OM are partially screened. Network formation decreases of SSA, resulting in less adsorption, while colloids branching increases the density of available binding sites, leading to an increase in adsorption. Investigating the REE adsorption mechanisms is thus crucial to comprehend the overall adsorption capability of the Fe-OM aggregates and their subsequent impact on REE mobility and transfer in the environment.

Our objective is to provide a detailed description of the parameters that control the Fe-OM aggregate as regard to REE. Aggregates of Fe-OM-Ca were synthesized with a constant Ca/Fe ratio of 0.5 (mol mol^{-1}) and various Fe/OC ratios (ranging from 0.1 to 0.0008 mol mol^{-1}). Adsorption experiments were carried out to investigate the distribution of REE relative to structure of the Fe-OM aggregates in order to evaluate the involved mechanisms and the controlling parameters. For this, experimental datasets were analysed to investigate the REE patterns variation relative to the REE concentrations, Fe/OM ratio, presence of Ca and pH. The surface interactions of REE with the Fe-OM aggregate was investigated by X-ray absorption spectroscopy (XAS), carried out at the Ce K-edge.

2. Materials and methods

2.1. Colloid synthesis

The colloids were synthesized with Leonardite humic acid (HA) (International Humic Substances Society) at Fe/OC ratios = 0.25 (mol mol^{-1}) and without or with Ca for Ca/Fe = 0.5 following the protocol of Guénet et al. [24] and Beauvois et al. [22,36,37]. The studied ratio were chosen in coherent with those reported for natural wetland by Dia et al. [38] and Pourret et al. [39]. Humic acids major elements are C = 63.81%, O = 31.27% as a mass fraction. All aqueous solutions were prepared with ultra-pure water (Milli-Q-Integral, Millipore). The samples were named with specific titles (Caxx-Feyy) and (Fexx-OMyy) according to Fe-OM and Ca-Fe ratios.

By HA titration with Fe(II) and Ca(II) solution for the Ca-containing colloids, the Fe-OM colloids were synthesized. The exact protocol is detailed by Guénet et al. [24]. The titration solution was prepared with $FeCl_4{\cdot}4H_2O$ (Sigma Aldrich) at 1000 mg L^{-1} of Fe(II) and $CaCl_2{\cdot}2H_2O$ (Sigma Aldrich) at 1000 mg L^{-1} of Ca(II).

The ionic strength (IS) of the titration and HA solutions were fixed at 5 mM with NaCl. The titration solution was added to a HA suspension at 700 mg L^{-1} at 0.05 mL min^{-1} using an automated titrator (Titrino 794, Metrohm). The pH was kept constant at 6.5 by adding NaOH 0.1 M. (Titrino 794, Metrohm). The pH measurement accuracy was ± 0.04 pH unit.

2.2. Adsorption experiments

Adsorption experiments of REE (Lanthanide, from La to Lu stock solution CCS-1, Inorganic Venture) by Fe-OM colloids were carried out at five REE/Fe molar ratios from 0.0008 to 0.1 as measured on natural samples collected from mining areas. The colloids suspensions were diluted 100 times without modifying the Fe/OM ratios. The dilution did not modify the colloids size and stability significantly as showed by DLS measurement (detailed results are provided in supplementary

information SI. 1).

REE adsorption by colloids was investigated using a common batch equilibrium method. After REE addition to the colloid's suspension, the pH was adjusted at pH 4 and 6 with HNO_3 and/or NaOH (0.1 to 1 mol L^{-1}). These pHs were chosen to obtain REE pattern at low and high REE loading (amount of adsorbed REE). The equilibrium time was 48 h as determined from previous studies [40].

At equilibrium, the suspensions were ultra-filtered at 3 kDa with Polyether sulfone membrane (PES) (Sartorius) and using ultrafiltration cells to separate REE bound to the colloids from the solution. The ultrafiltration cells were washed with 0.05 M HNO_3 and 3 times with ultrapure water to reach a total dissolved organic carbon concentration under 0.2 mg L^{-1}. After ultrafiltration, all samples were acidified with 0.37 mol L^{-1} HNO_3 before ICP-MS measurements.

REE complexation with colloids is described using the apparent partition coefficient K_d relative to the dissolved organic carbon (DOC), as follow:

$$K_d(ln) = \frac{[ln_{adsorbed}]\mu gL^{-1}/gDOC}{[ln^{3+}]\mu gL^{-1}} \quad (1)$$

where ln = La to Lu.

The pattern evolution relative to the experimental conditions was highlighted using the La/Sm ratio that fingerprint the MREE downward concavity modification and the Gd/Yb ratio that fingerprint the LREE increase or decrease. Both were calculated using the log K_d(ln).

2.3. Chemical analysis

Total organic carbon (TOC) was measured using a TOC-V Shimadzu analyser, the accuracy of measurement was ±5% as determined by using a standard solution of potassium hydrogen phthalate (Sigma Aldrich).

The concentrations of Fe, Ca and REE were measured using a QQQ-ICP-MS instrument (Agilent Technologies-8,900), features two quadrupole mass filters and has greater sensitivity and smaller backgrounds than single quadrupole ICP-MS, which facilitates analysis of particulate pollutants. Calibration curves were generated and validated with certified reference materials (SLRS-6, National Research Council). A rhodium solution was used as an internal standard to correct for instrumental drift and possible matrix effects. The average limit of quantification of REE was calculated by measuring 10 blank samples. After averaging the standard deviation (SD), the limit of quantification (LOQ) was calculated using the following formula: (Eq. 2) LOQ = 10 × SD and was considered to be 0.1 ppt. Since the upper limit of the REE calibration curve was 5 ppb, samples were diluted so that this value was not exceeded.

Dynamic light scattering was used to verify the effects of dilution on colloids (VASCO Flex, Cordouan Technologies), details of the methodology are provided in SI- Table S1.

2.4. X-ray absorption spectroscopy

X-Ray Absorption Spectroscopy (XAS), including X-ray Absorption Near Edge Spectroscopy (XANES) and Extended X-ray Absorption Fine Structure (EXAFS), was performed to identify the atomic neighbouring of REE when adsorbed by Fe-OM colloids. Since the adsorption edges of REE are close to each other, it is impossible to record EXAFS when the whole REE group is present. We therefore chose to study only Ce notably because of its potential to be oxidized by Fe-oxides [41,42]. Cerium(III) was adsorbed at a Ce/Fe ratio = 0.1 mol mol^{-1} onto the 0.25 Fe-OM colloids without and with Ca (Ca/Fe ratio = 0.5) at pH 7 and IS = 5 mmol L^{-1} of NaCl. The Ce L3-edge XANES and EXAFS spectra (5723 eV) were record at the Synchrotron SOLEIL on the LUCIA beamline (SOLEIL, St Aubin, France) [43,44]. A Si(1 1 1) double crystal was used as monochromator. The monochromator was calibrated by setting the initial inflexion point of a Cr metallic foil XANES to 5987 eV, the beam size was 2 × 2 mm^2. Measurements were performed in fluorescence mode (using a Bruker 60 mm2 mono-element SDD) and in transmission (using a silicon diode) when possible. The reference compounds (CeO_2 and $Ce(SO_4)_3$) were prepared as pellets of finely ground and homogenized powder combined with cellulose. The Ce adsorbed Fe-OM aggregates samples (Ce-Fe-OM, Ce-Fe-OM-Ca), were crushed on indium foil. All the samples were analysed under vacuum at 25 K, using a liquid helium cryostat to prevent any beam-induced redox damages. EXAFS spectra were collected with steps of 3 eV in the pre-edge region (5650–5710 eV), 0.5 eV in the edge region (5711–5790 eV), and 2 eV in the post-edge region (5791–6100 eV), with a counting time of 1 s $step^{-1}$. For each sample, the recorded spectra (up to four) were superimposed, demonstrating that no beam damage had occurred as a result of these measurement conditions.

XANES and EXAFS spectra were extracted using the Athena software [45] including the Autbk algorithm (Rbkb = 1, K-weight = 3). Normalized spectra were obtained by fitting the pre-edge region with a linear function and the post-edge region with a quadratic polynomial function.

EXAFS spectra were analysed by shell fitting. A theoretical back scattering paths were calculated from the crystal structure of Ce $(HCOO)_3$ [46]. Theoretical phase and amplitude functions were calculated using FEFF. The paths were carefully considered and selected for the final fits using the Artemis software [45]. The Fourier transform of the k^3-weighted EXAFS spectra were calculated over a range of 2–9 $Å^{-1}$ using an Hanning apodization window (window parameter = 1). The shell fits were performed on the 1–5 Å range of the FTs k^3-weighted spectra. The amplitude reduction factor was set to 0.9. The number of O was fixed to 9 throughout the data fits as performed by Henning et al. 2013.

3. Results

3.1. Rare earth elements adsorption patterns

The patterns of the distribution coefficient (Log K_d) of REE bound to colloids with and without Ca were plotted relative to the REE/Fe ratios in Figs. 1 and 2 for Fe/OM 0.25 at pH 6 and 4, respectively. All REE patterns varied with the REE/Fe ratios, namely with the REE concentrations and thus REE loading. At pH 6, for high REE concentration and high loading (i.e. REE/Fe ≥ 0.05), REE patterns exhibited a typical middle REE downward concavity, typical of the REE binding to OM as previously reported [34,47,48] (Fig. 1A). More importantly, at low REE concentration and loading (i.e. REE/Fe ≤ 0.0129), patterns exhibited a non-common enrichment of light REE (LREE) and a depletion of heavy REE (HREE) as illustrated by the increasing La/Sm ratios (Fig. 1B). When the REE are adsorbed on the MO, the pattern exhibits an enrichment in LREE at low loading that evolves to a MREE downward concavity at high loading [48,49]. When adsorbed on the surface of Fe oxyhydroxides, a tetrad effect, sometimes a positive Ce anomaly and a strong MREE downward concavity, due to the low La adsorption, are developed [41,50]. An enrichment in LREE is never observed for both phases. Moreover, up to our knowledge, such patterns have never been observed in natural water [20,21,51,52]. However, at low REE loading, the fraction < 3 kDa exhibited a REE pattern with a MREE downward concavity and an enrichment in HREE (exact inverse of the REE patterns of the >3 kDa fraction) (SI, Figure S1 A and B) and a DOC concentration at around 0.3 mg L^{-1}, indicating that small organic colloids have passed through membrane. In presence of OM, this typical REE pattern was previously attributed, for low REE loading, to the binding of REE by OM as multidentate or phenolic complexes [48]. All these results suggested that, at pH 6, small organic colloids (size < 3 kDa) have preferentially bound REE as strong complexes, imposing an inverse pattern on the solution > 3 kDa. Note, however, that only 0.9 % of ΣREE are released from the Fe-OM colloids with these organic colloids < 3 kDa. The presence of Ca seems to not modify significantly both the REE adsorbed

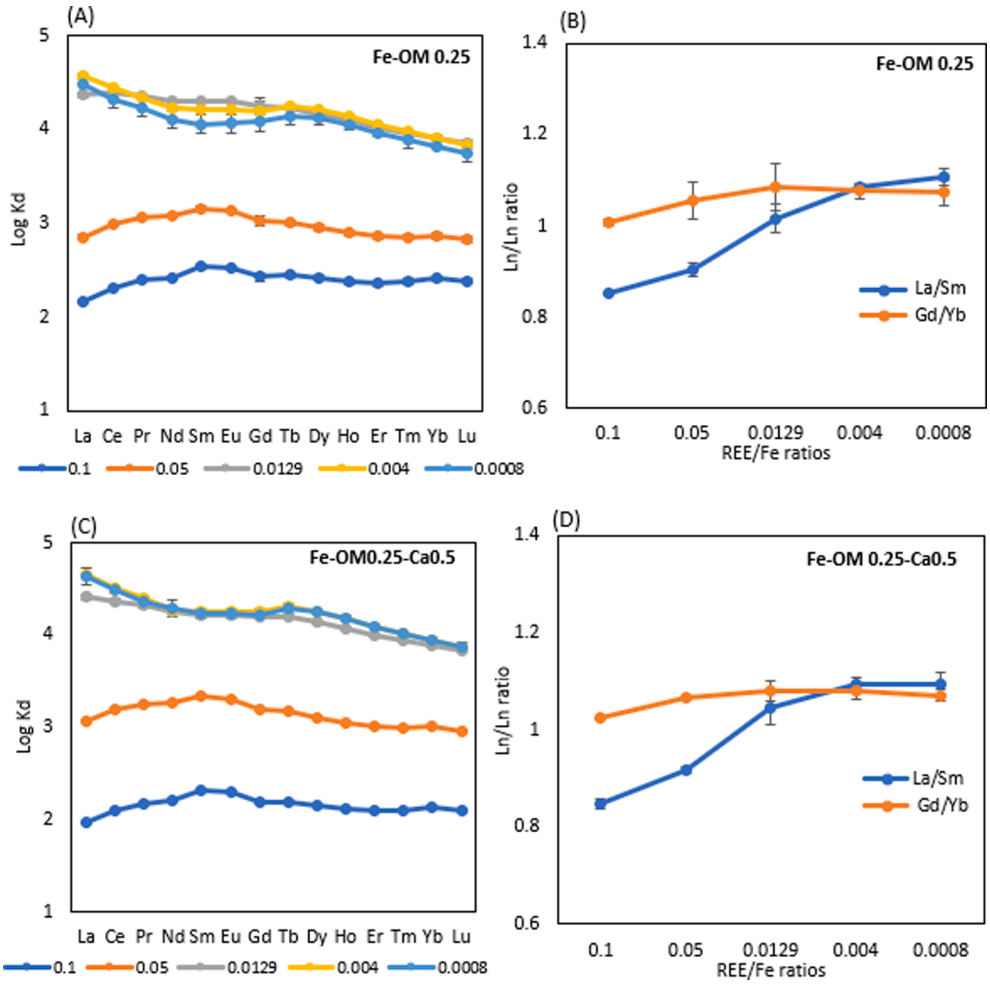

Fig. 1. Variation of Log K_d^{REE} patterns relative to the REE/Fe ratios (0.1, 0.05, 0.0129, 0.004, 0.0008) at Fe/OM 0.25, without (A) and with Ca (C) and evolution of La/Sm and Gd/Yb ratios relative to REE/Fe without (B) and with Ca (D) at pH = 6. Error bars represent triplicates of experiments.

amount and patterns as shown by comparison of the Fig. 1(A) and (C).

At pH 4 without Ca, the log K_d was lower than those at pH 6 indicating a smaller amount of bound REE (Fig. 2A). A MREE downward concavity was observed for all REE loadings that decreased with the decreasing REE loading in response to the increasing La adsorption as compared to Sm (Fig. 2 A and B). No significant HREE variations were observed (Fig. 2 A and B). At pH 4, no small organic colloids pass thus through the 3 kDa membrane. At pH 4, most binding sites are protonated limiting the adsorption of REE and the formation of multidendate complexes. Complexation with phenolic sites is limited since they are all protonated (pKa φ-OH ≈8) [53]. Therefore, acidic pH limits the release of REE complexes with small organic colloids and the REE adsorption as strong complex, avoiding a significant variation of the REE pattern with the REE loading. With Ca, the patterns were flatter with a less marked MREE downward concavity and no HREE variations as demonstrated by the very small variation of La/Sm and Gd/Yb ratios (Fig. 2C and D).

3.2. REE adsorption isotherms

Lanthanum, Eu and Yb adsorption isotherms are plotted for the 0.25 Fe-OM ratio with and without Ca at pH 6 and 4 in Fig. 3. At pH 6 without Ca, La, Eu and Yb adsorbed concentrations increased with the increasing free REE concentrations without reaching a plateau. Adsorption isotherms can be divided in two parts. For free La, Eu and Yb $< 10^{-2}$ mg L^{-1}, adsorption increased strongly with the free concentration. Over this value, adsorption increased weakly suggesting a progressive saturation of the surface even if no plateau was reached. Lanthanum was more adsorbed than Eu which is more adsorbed than Yb. At pH 6 with Ca, lower amount of La, Eu and Lu are adsorbed (log K_d values are lower with Ca, Fig. 2 C and D). The inflection concentration of the isotherm was around 5×10^{-3} mg L^{-1}, namely 2 time smaller than without Ca. Such result indicated a progressive site saturation, reached at lowest concentration than without Ca. Moreover, a pseudo equilibrium seemed to be reached for La (Fig. 3 B). All these results suggest an impact of the Ca on the binding mechanism of REE by the Fe-OM colloids.

At pH 4 without Ca, La, Eu and Yb adsorbed concentrations were strongly lower than at pH 6 (6 against 16 mg L^{-1} for La at pH 4 and 6, respectively). This decrease can be explained by the increase of the protonated OM sites as well as the OM aggregation that limit the binding site availability [54]. The isotherms were also quite different than at pH 6. Without Ca, if Isotherm can be divided in two parts, the first part that corresponded to the strongest adsorption, have a lower slope (0.32) indicating a lowest adsorption than at pH 6. From 5×10^{-2} mg L^{-1} a pseudo plateau seemed to be reached. These results demonstrated that pH 4 strongly limit the REE adsorption onto the Fe-OM colloids and that a site saturation was reached. With Ca, adsorption isotherm exhibited the same slope (0.32) and no plateau seemed to be reached. However, the max of adsorption is the same for experiment with and without pH (ex. for La, $adsorbed_{max}$ was equal to 6.9 mg g^{-1} without Ca against 6.6 mg g^{-1} with Ca). Therefore, at pH 4 for this Ca concentration, the presence of Ca seems have no influence on the sorption processes.

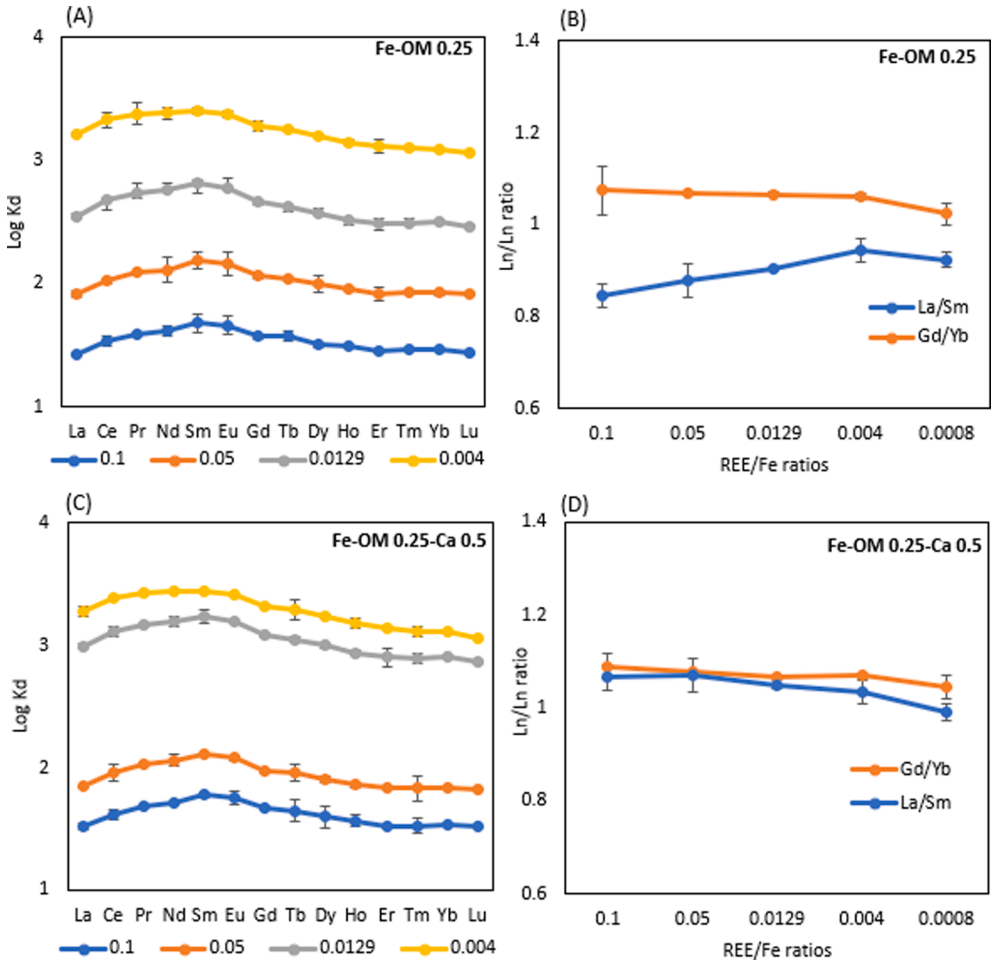

Fig. 2. Variation of Log K_d^{REE} patterns relative to the REE/Fe ratios (0.1, 0.05, 0.0129, 0.004) at Fe/OM = 0.25, without (A) and with Ca (C) and evolution of La/Sm and Gd/Yb ratios relative to REE/Fe without (B) and with Ca (D) at pH = 4. Error bars represent triplicate of experiments.

3.3. X-ray-absorption microscopy

The oxidation state of Ce in Ce-Fe-OM samples with and without Ca was determined from XANES spectra collecting at the Ce L_{III}-edge. The spectra of both Ce-Fe-OM colloids with or without Ca and that of the Ce (III) reference are reported in Fig. 4. The spectra shapes demonstrated a noticeable difference between trivalent and tetravalent Ce, namely that Ce(III) exhibits a single sharp peak around 5727 eV followed by a broad oscillation around 5760 eV while Ce(IV) exhibits a two-humped peak at 5731 and 5738 eV respectively followed by a broad oscillation at 5770 eV.

The white line maximum of the 2 samples at 5726.82 eV matched with that of the Ce(III) reference, and is followed by a broad band centred around 5760 eV. These results demonstrated that Ce was present as Ce(III) in both Ce-Fe-OM colloids and that no oxidation seemed to occur in these samples. However, several studies suggested that Fe-oxyhydroxide has the possibility to catalysis the oxidation of Ce(III) as Ce(IV) [41,42]. By contrast, from Ce L_{III}-edge XAS analysis of a Ce-ferrihydrite, Nakada et al. (2013) and Yu et al. (2017) showed that Ce adsorbed on ferrihydrite exists predominantly as trivalent species, and no oxidation of Ce(III) as Ce(IV) occurred at the ferrihydrite surface under their physico-chemical conditions (pH 5 and 6.4 and Ce/Fe ratio = 0.1). However, Yu et al. (2017), observed a modest shoulder at 5737 eV on their XANES spectra that could correspond to a small amount of Ce (IV).

The EXAFS and the corresponding Fourier-Transform (FTs) of the Fe-OM colloids with and without Ca are reported in Fig. 5. The EXAFS spectra of both samples were quite similar, monotonously oscillating with a shoulder occurring at 6 $Å^{-1}$ which has a higher intensity in presence of Ca. Three peaks dominated the FT. The first peak located at 2.2 Å (R + ΔR), corresponded to the first shell of neighboring atoms around the Ce. The scattering of the Ce neighbors from the second and third coordination shells led to the formation of the second and third peaks, which were respectively measured at 2.8 and 3.5 Å (R + ΔR). The first intense peak at 2.2 Å was well reproduced with the backscattering signal of 9O first neighbors at 2.51 Å. The peak at 2.8 Å was fitted by adding C as second neighbor at 3.25 Å (Table 1).

The present result clearly demonstrated that no oxidation of Ce(III) as Ce(IV) occurred at the surface of the Fe-OM colloids. Moreover, the fitting of the EXAFS data demonstrated that the second neighbour of Ce at the surface of the colloids is C. All these results suggested that Ce and thus REE could not be bound to the Fe nanoparticles or oligomer constitutive of the colloids but rather to their OM part.

4. Discussion

The REE patterns at the Fe-OM colloids surface mainly varied with the pH and REE loading (Fig. 1). X-ray absorption spectroscopy demonstrated that REE were bound to the OM component of the Fe-OM colloids. This result is also supported by the absence of a Ce positive anomaly development on the REE patterns that can be observed relative to the physico-chemical conditions for the pattern of REE adsorbed onto Fe-oxyhydroxides [41]. The variation of the REE pattern is therefore only controlled by the OM behavior relative to the pH conditions.

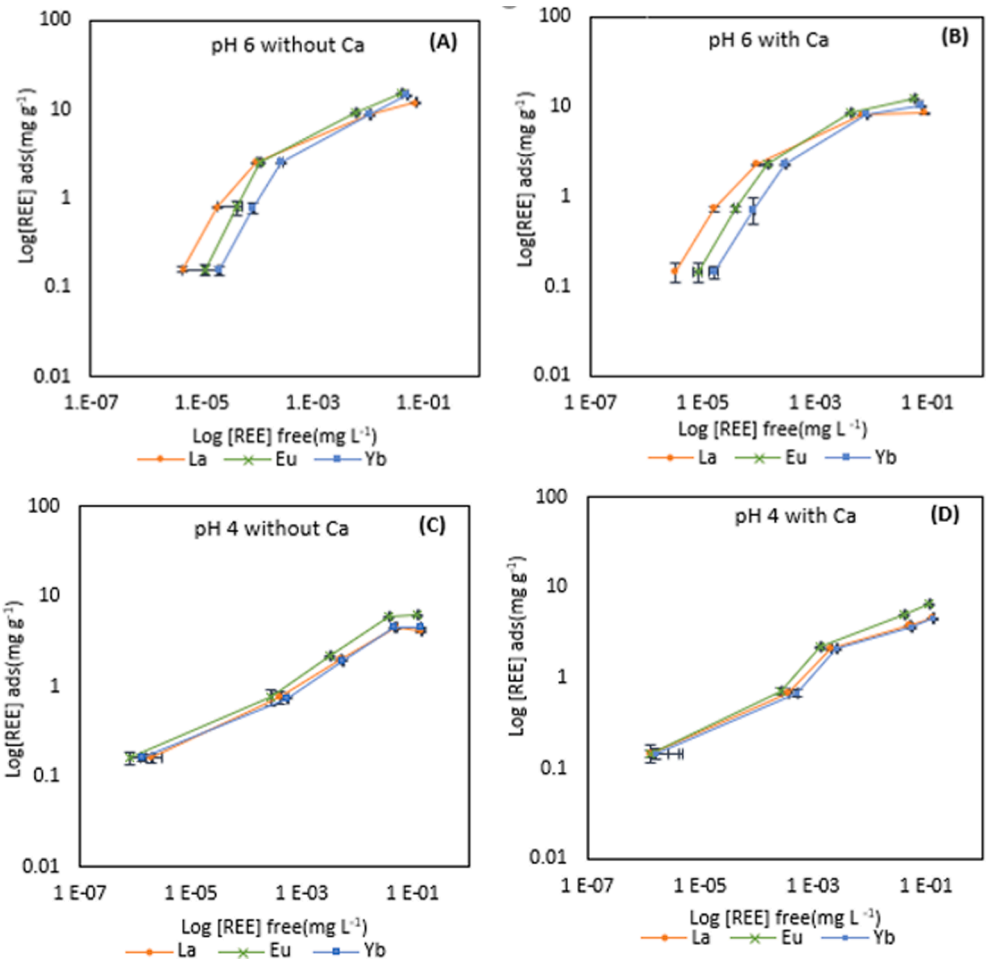

Fig. 3. Adsorption isotherm of La, Eu and Yb at Fe/OM 0.25 ratios and 0.1,0.05,0.0129,0.004 and 0.0008 REE/Fe ratios without (A) and with Ca (B) at pH 6, without (C) and with Ca (D) at pH 4.

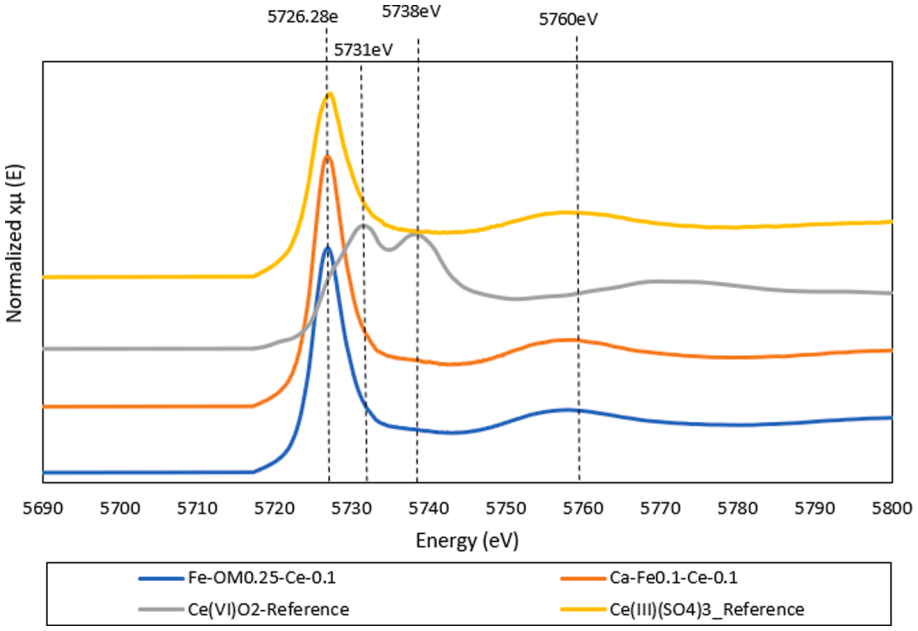

Fig. 4. Ce L_{III}-edge XANES spectra for samples and relevant references.

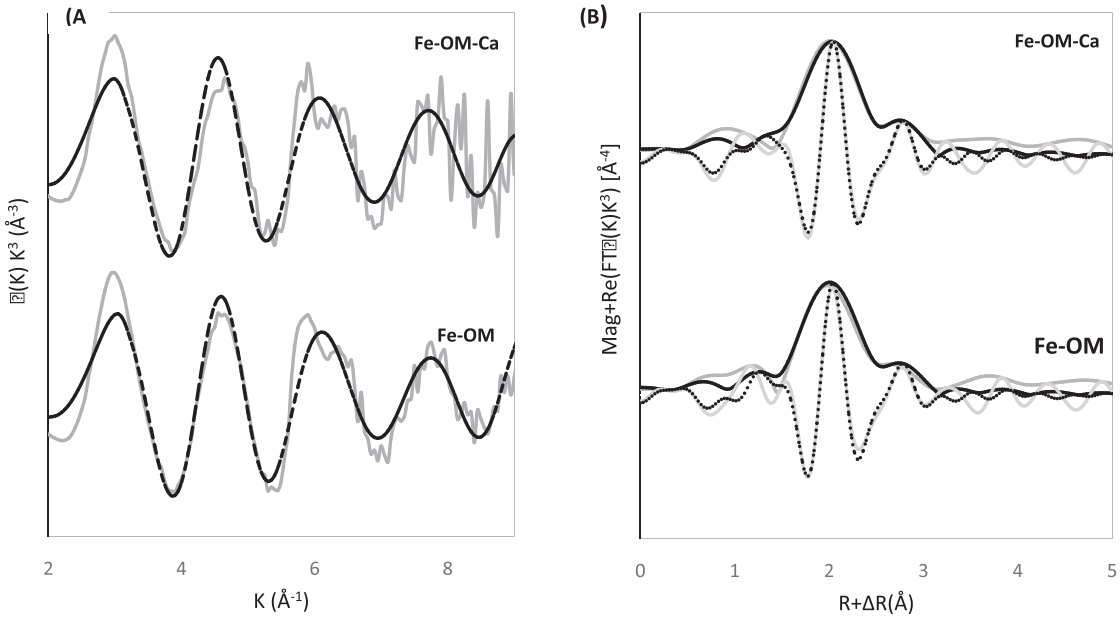

Fig. 5. (A) Cerium L_{III}-edge EXAFS spectra for the Fe-OM-Ca and Fe-OM colloids (B) the magnitude and imaginary part of the associated Fourier Transform, not corrected from phase shift. Solid lines are experimental data and dotted lines are the fit results.

Table 1
EXAFS Fit Parameters of Fe-OM-Ce and Fe-Ca-OM-Ce for Ce/Fe ratio = 0.1, Fe-OM 0.25 and Ca/Fe ratio = 0.5 at pH 6 and IS 5 mmol L^{-1} of NaCl. E0 was set to 5.24 eV, S02 to 0.

Sample	Path	N	R	SS^2	E_0 (eV)	Reduced X^2	R-factor
Fe/OM 0.25 Ce/Fe 0.1	Ce-O	9.0[a]	2.51	0.012	5.24	72.7	0.07
	Ce-C	3.3	3.25	0.006	–	–	–
Fe/OM 0.25-Ca 0.5	Ce-O	9.0[a]	2.51	0.012	5.24	32	0.08
Ce/Fe 0.1	Ce-C	3.3	3.25	0.005	–	–	–

[a] Coordination numbers are taken from the crystallographic data of Ce(COOH)3 [46] and fixed during the fit procedure. Errors in R distances are ±1%, errors in coordination numbers are ±10% error on sigma ss ±20%.

The most important variation was obtained at pH 6 for the lower REE concentrations and loading. As previously stated, these patterns are controlled by the fractionation of the OM colloids occurring at pH 6 and resulting in the release of small organic colloids from the supramolecular structure of the whole OM [55]. Under our experimental conditions, these small organic colloids with their REE loading were physically separated from the whole OM colloids thanks to the ultrafiltration membrane (fraction < 3 kDa). The amount of REE adsorbed to this small organic colloid was low (0.012 µg L^{-1}). As previously explained by Marsac et al. (2010), at low REE loading, REE preferentially form strong multidendate or phenolic complexes with OM which result in a REE pattern exhibited a strong HREE enrichment as observed here at pH 6 in the fraction < 3 kDa. Because the REE concentration were low, the REE binding as strong complexes to the small colloids (combined with the K_d REE calculation effect) control the REE pattern of the fraction > 3 kDa. However, when the REE concentration increased, REE were bound not only as strong complexes (multidendate and phenolic) but also as weaker bidentate complexes with the most abundant COOH sites of the OM [48]. These complexes become progressively dominants with the increasing REE loading. As a result, the HREE enrichment disappeared since masked by the MREE downward concavity produced by the REE binding to the weak but abundant COOH sites of OM.

At pH 4, the MREE downward concavity was observed regardless of the REE concentrations and loadings indicating that the REE-COOH-OM binding dominate for all experimental conditions although the concentration of adsorbed REE was lower than at pH 6. But, by contrast with pH 6 that involved the fractionation of the whole OM colloids, pH 4 promotes its aggregation [12,13,55], avoiding the release of small colloids and molecules and therefore the pattern control by the strong but less abundant REE multidendate/phenolic complexes.

This different mechanisms at pH 6 and pH 4 explain the difference obtained for the REE adsorption isotherms. At pH 6, isotherm was more curved and can be divided into two parts from 5×10^{-2} mol L^{-1} free REE. This concentration corresponds to the concentration when the REE binding as bidendate complexes with the –COOH sites become dominant, in response to the OM pH-fractionation. By contrast, the isotherm at pH 4 is not controlled by the formed complexes (since OM is aggregated and no fractionation occurred) but rather by the total amount of adsorbed REE.

The influence of Ca on the REE adsorption seems to be low and rather insignificant at pH 4. At pH 6, isotherm suggested that Ca may limit the REE adsorption on the OM part of the Fe-OM colloids. Beauvois et al. (2020) demonstrated that when the Fe-OM colloids are synthesized with Ca, Ca was only bound to the OM and not to the iron phases. Calcium is bound to the COOH OM site, connecting the OM molecules and colloids to form a large network at high concentration of Ca [22]. In our experimental conditions, REE and Ca could therefore compete for their binding to the OM of the Fe-OM colloids which results in a slight decrease of the REE adsorbed amount.

4.1. *Impact of the colloid dynamic on the REE mobility*

Understanding how REEs are transported throughout the environment is one of the first steps toward preventing the health hazards associated with them. Here, we demonstrated that since REE are mainly bound to the OM of the Fe-OM colloids, their fate and their subsequent mobility and transfer will be only controlled by the OM behavior and interactions with the Fe phases and other competitive elements. According to previous research, the aggregation of OM is dynamic, especially with reference to pH (Pédrot et al., 2010). At acidic pH, the amount of REE bound to the Fe-OM colloids is low and pH involves OM aggregation and result in an increase of the Fe-OM colloids size [56,57]

which can limits their mobility and transfer as well as that of adsorbed REE in porous media such as soil and sediment. By contrast, at higher pH, the aggregation is lower. The COOH groups are progressively protonated increasing the repulsion between organic molecules/colloids. However, at pH 4, some H bonding that remained, combined with the Fe phases occurrence, maintain a degree of aggregation that result in the release of a limited quantity of tiny colloids. Kloster et al; (2013) estimated that fractionation of humic substances can occur only down to 60% of aggregation [58]. The result is that only 0.9 % of ΣREE are released from the Fe-OM colloids with this tiny organic colloid. This percentage is sufficient to control the log K_{dREE} pattern in our experimental conditions notably due to the log K_{dREE} calculation mode. This fractionation will thus influence the REE mobility only regarding to the amount of this tiny OM colloids that can be produced under the prevailing environmental conditions. At pH 6, the size of the OM and subsequently of the entire Fe-OM colloids decrease while complexing high amount of REE (between 90 and 99 % with the decreasing REE concentration). In such conditions, the mobility/transfer of REE will depend on the ability of the colloids to be water-transferred in the soil porosity or in surface water relative to the physico-chemical conditions.

A last important point is the impact of the major ion that influence the colloid structural organization, and/or compete with REE for their binding by OM. Beauvois et al. (2020) demonstrated that at pH 6.5, the size of OM inside the Fe-OM colloids significantly increases from Ca/OC = 0.026 (mol mol^{-1}) until forming an OM micrometric network that finally settled bringing with it the initially bound Fe phases. Before Ca/OC = 0.026, the OM size is around 400 nm and the Fe-OM aggregate behave as colloid, namely are stable in solution. Here Ca/OC = 0.5 (mol mol^{-1}), Fe-OM aggregate was thus stable in solution, and its sole influence is its low competition with REE. In these conditions, this competition is only possible since Ca is present as major ion although REE are as trace elements. Rare earth elements as metallic element and trivalent ion have indeed larger affinity for the carboxylic sites than Ca (log K REE-COOH is in the range of 2.55–2.84 and log K Ca-COOH = 1.18)[59]. Therefore, the impact Fe-OM aggregates will only significantly influence the REE mobility and transfer for high Ca/OC ratio when Ca can involve the formation of a micrometric network. Beauvois et al. (2023) also studied the impact of Al as major ion on the Fe-OM structural arrangement. They demonstrated that at pH 6.5, Al form monomers/oligomers that polymerized which branch out the OM and Fe aggregates resulting in a large settling network [37]. In such conditions, Al will have the same impact on the REE mobility/transfer than Ca.

Hence, the most important factors affecting the REE mobility/transfer is the parameter that modify the colloids conformational structure with respect to pH, and major ion concentration. The REE bound to Fe-OM colloids are thus expected to be immobilized by the colloid settlement and in soil and sediment, by the colloids trapping by the porosity. The challenge today is thus how the REE reactivity is controlled by the organo-mineral colloids structural arrangement relative to the prevailing physico-conditions.

5. Conclusion

Evaluating the mobility/transfer of REE in this environment is crucial to determine their environmental impact and the potential to be transfer between the various environmental compartment (water, soil, biota). The present study focused on the potential of the Fe-OM aggregates to bind and subsequently control the REE mobility and transfer. The choice of Fe-OM aggregate is justified by 1) the high binding affinity of REE for both Fe phases [41,50] and OM [40,49,60,61], 2) the ubiquity and increasing environmental production of Fe-OM aggregate with the climatic global changing and 3) the well-known structure of such aggregates [22–24,36,37]. Rare earth elements adsorption experiments by Fe-OM aggregate without and with Ca were thus carried out at pH 4 and 6. Rare earth element adsorption pattern combined with Ce-L_{III} edge XAS experiments showed that REE were only bound to the OM component of the Fe-OM aggregates which demonstrate that REE fate is only control by OM in the Fe-OM aggregates. As expected, the amount of the REE adsorbed increased with the increasing pH in response to the OM binding site deprotonation. The pH also controls the aggregation/disaggregation and size of the OM part of the Fe-OM colloids. This control result, at pH 6, in the release of tiny OM colloids (size < 3 kDa) in which REE form strong multidendate and/or phenolic complexes. However, they only complex 0.8% of the initial REE concentration. The impact of this tiny colloids on the REE mobility and transfer will thus depend on the quantity that can be produced as regards to the prevailing environmental conditions. But, pH 6 also promote the decrease of the Fe-OM size that will increase their mobility and those of the REE. By contrast, at pH 4, as demonstrated in the literature, the size of the OM colloids increases and potentially limits its mobility/transfer and those of REE. However, at pH 4, 4 time more REE remain soluble in solution as compared to pH 6 (amount of adsorbed REE 4.4 mg g^{-1} at pH 4 against 12 mg g^{-1}). Therefore, while the Fe-OM size increase, pH will globally promote the REE mobility.

In the studied experimental conditions, the impact of Ca was low and can only be observed at pH 6. The Ca impact only occurred through its competition with REE for its binding to the OM COOH groups and since occurring as major ion. At pH 4, no impact of Ca was notified although its high concentration, Ca was unable to compete with REE for the lower quantity of deprotonated COO– groups. However, as demonstrated in the literature for pH 6.5, for higher concentration Ca as well as other major ions as Al, a micrometric OM network can occur and result in the Fe-OM settlement that will immobilized REE.

Therefore, the mobility and transfer of REE when interacting with Fe-OM aggregates is mainly controlled by the pH that controls 1) the REE adsorbed amount, 2) the size of the aggregate and its subsequent mobility in porous media 3) and indirectly the amount of major ions that are allowed to bind to OM and to polymerize in order to form a micrometric network that result in the Fe-OM aggregates settlement in the porous media or in the water flow.

CRediT authorship contribution statement

Yasaman Tadayon: Conceptualization, Methodology, Investigation, Data curation, Formal analysis, Software, Writing – original draft. **Delphine Vantelon:** Supervision, Investigation, Data curation, Software, Writing – review & editing. **Julien Gigault:** Supervision, Data curation, Writing – review & editing, Visualization. **Aline Dia:** Writing – review & editing. **Maxime Pattier:** Resources, Formal analysis, Data curation. **Lionel Dutruch:** Resources, Formal analysis, Data curation. **Mélanie Davranche:** Supervision, Validation, Writing – review & editing, Project administration.

Declaration of competing interest

The authors declare that they have no known competing financial interests or personal relationships that could have appeared to influence the work reported in this paper.

Data availability

No data was used for the research described in the article.

Acknowledgements

This project has received funding from the European Union's Horizon 2020 research and innovation program under the Marie Sklodowska-Curie Grant Agreement No 857989.

Appendix A. Supplementary data

Supplementary data to this article can be found online at https://doi.org/10.1016/j.jcis.2023.10.110.

References

[1] S. Lawrence, P. Davies, G. Hil, I. Rutherfurd, J. Grove, J. Turnbull, E. Silvester, F. Colombi, M. Macklin, Characterising mine wastes as archaeological landscapes, Geoarchaeology (2023).

[2] I. Bortone, H. Sakar, A. Soares, Gaps in Regulation and Policies on the Application of Green Technologies at Household Level in the United Kingdom, Sustainability 14 (2022), https://doi.org/10.3390/su14074030.

[3] G. Pitron, The war for rare earth metals-The hidden face of the energy and digital transition, 2018.

[4] Z. Hu, H. Richter, G. Sparovek, E. Schnug, Physiological and biochemical effects of rare earth elements on plants and their agricultural significance: a review, J. Plant Nutr. 27 (2004) 183–220.

[5] M. Bau, A. Knappe, P. Dulski, Anthropogenic gadolinium as a micropollutant in river waters in Pennsylvania and in Lake Erie, northeastern United States, Geochemistry 66 (2006) 143–152, https://doi.org/10.1016/j.chemer.2006.01.002.

[6] R.K. Jyothi, T. Thenepalli, J.W. Ahn, P.K. Parhi, K.W. Chung, J.-Y. Lee, Review of rare earth elements recovery from secondary resources for clean energy technologies: Grand opportunities to create wealth from waste, J. Clean. Prod. 267 (2020), 122048, https://doi.org/10.1016/j.jclepro.2020.122048.

[7] G. Gaustad, E. Williams, A. Leader, Rare earth metals from secondary sources: Review of potential supply from waste and byproducts, Resour. Conserv. Recycl. 167 (2021), 105213, https://doi.org/10.1016/j.resconrec.2020.105213.

[8] D.H. Dang, K.A. Thompson, L. Ma, H.Q. Nguyen, S.T. Luu, M.T.N. Duong, A. Kernaghan, Toward the circular economy of Rare Earth Elements: a review of abundance, extraction, applications, and environmental impacts, Arch. Environ. Contam. Toxicol. 81 (2021) 521–530.

[9] G. Pagano, P.J. Thomas, A. Di Nunzio, M. Trifuoggi, Human exposures to rare earth elements: Present knowledge and research prospects, Environ. Res. 171 (2019) 493–500, https://doi.org/10.1016/j.envres.2019.02.004.

[10] S. Kulaksız, M. Bau, Contrasting behaviour of anthropogenic gadolinium and natural rare earth elements in estuaries and the gadolinium input into the North Sea, Earth Planet. Sci. Lett. 260 (2007) 361–371.

[11] Q. Liu, H. Shi, Y. An, J. Ma, W. Zhao, Y. Qu, H. Chen, L. Liu, F. Wu, Source, environmental behavior and potential health risk of rare earth elements in Beijing urban park soils, J. Hazard. Mater. 445 (2023), 130451, https://doi.org/10.1016/j.jhazmat.2022.130451.

[12] J. Buffle, G.G. Leppard, Characterization of Aquatic Colloids and Macromolecules. 1. Structure and Behavior of Colloidal Material, Environ. Sci. Technol. 29 (1995) 2169–2175, https://doi.org/10.1021/es00009a004.

[13] J. Buffle, G.G. Leppard, Characterization of Aquatic Colloids and Macromolecules. 2. Key Role of Physical Structures on Analytical Results, Environ. Sci. Technol. 29 (1995) 2176–2184, https://doi.org/10.1021/es00009a005.

[14] N.S. Wigginton, K.L. Haus, M.F. Hochella Jr, Aquatic environmental nanoparticles, J. Environ. Monit. 9 (2007) 1306–1316.

[15] H. Guénet, M. Davranche, D. Vantelon, M. Pédrot, M. Al-Sid-Cheikh, A. Dia, J. Jestin, Evidence of organic matter control on As oxidation by iron oxides in riparian wetlands, Chem. Geol. 439 (2016) 161–172.

[16] E. Lotfi-Kalahroodi, A.-C. Pierson-Wickmann, H. Guénet, O. Rouxel, E. Ponzevera, M. Bouhnik-Le Coz, D. Vantelon, A. Dia, M. Davranche, Iron isotope fractionation in iron-organic matter associations: Experimental evidence using filtration and ultrafiltration, Geochim. Cosmochim. Acta 250 (2019) 98–116.

[17] G. Ratié, D. Vantelon, E.L. Kalahroodi, I. Bihannic, A.-C. Pierson-Wickmann, M. Davranche, Iron speciation at the riverbank surface in wetland and potential impact on the mobility of trace metals, Sci. Total Environ. 651 (2019) 443–455.

[18] O.S. Pokrovsky, B. Dupré, J. Schott, Fe–Al–organic colloids control of trace elements in peat soil solutions: results of ultrafiltration and dialysis, Aquat. Geochem. 11 (2005) 241–278.

[19] L.K. ThomasArrigo, C. Mikutta, J. Byrne, K. Barmettler, A. Kappler, R. Kretzschmar, Iron and arsenic speciation and distribution in organic flocs from streambeds of an arsenic-enriched peatland, Environ. Sci. Technol. 48 (2014) 13218–13228.

[20] C. Hirst, P.S. Andersson, S. Shaw, I.T. Burke, L. Kutscher, M.J. Murphy, T. Maximov, O.S. Pokrovsky, C.-M. Mörth, D. Porcelli, Characterisation of Fe-bearing particles and colloids in the Lena River basin, NE Russia, Geochim. Cosmochim. Acta 213 (2017) 553–573.

[21] O.S. Pokrovsky, J. Schott, Iron colloids/organic matter associated transport of major and trace elements in small boreal rivers and their estuaries (NW Russia), Chem. Geol. 190 (2002) 141–179.

[22] A. Beauvois, D. Vantelon, J. Jestin, C. Rivard, M. Bouhnik-Le Coz, A. Dupont, V. Briois, T. Bizien, A. Sorrentino, B. Wu, M.-S. Appavou, E. Lotfi-Kalahroodi, A.-C. Pierson-Wickmann, M. Davranche, How does calcium drive the structural organization of iron–organic matter aggregates? A multiscale investigation, Env. Sci. Nano 7 (2020) 2833–2849, https://doi.org/10.1039/D0EN00412J.

[23] L. Gentile, T. Wang, A. Tunlid, U. Olsson, P. Persson, Ferrihydrite Nanoparticle Aggregation Induced by Dissolved Organic Matter, J. Phys. Chem. A 122 (2018) 7730–7738, https://doi.org/10.1021/acs.jpca.8b05622.

[24] H. Guénet, M. Davranche, D. Vantelon, J. Gigault, S. Prévost, O. Taché, S. Jaksch, M. Pédrot, V. Dorcet, A. Boutier, Characterization of iron–organic matter nano-aggregate networks through a combination of SAXS/SANS and XAS analyses: impact on As binding, Environ. Sci. Nano 4 (2017) 938–954.

[25] C. Poggenburg, R. Mikutta, M. Sander, A. Schippers, A. Marchanka, R. Dohrmann, G. Guggenberger, Microbial reduction of ferrihydrite-organic matter coprecipitates by Shewanella putrefaciens and Geobacter metallireducens in comparison to mediated electrochemical reduction, Chem. Geol. 447 (2016) 133–147, https://doi.org/10.1016/j.chemgeo.2016.09.031.

[26] M. Pédrot, A.L. Boudec, M. Davranche, A. Dia, O. Henin, How does organic matter constrain the nature, size and availability of Fe nanoparticles for biological reduction? J. Colloid Interface Sci. 359 (2011) 75–85, https://doi.org/10.1016/j.jcis.2011.03.067.

[27] D. Vantelon, M. Davranche, R. Marsac, C. La Fontaine, H. Guénet, J. Jestin, G. Campaore, A. Beauvois, V. Briois, Iron speciation in iron–organic matter nanoaggregates: a kinetic approach coupling Quick-EXAFS and MCR-ALS chemometrics, Env. Sci. Nano 6 (2019) 2641–2651, https://doi.org/10.1039/C9EN00210C.

[28] C. Chen, J.J. Dynes, J. Wang, D.L. Sparks, Properties of Fe-Organic Matter Associations via Coprecipitation versus Adsorption, Environ. Sci. Technol. 48 (2014) 13751–13759, https://doi.org/10.1021/es503669u.

[29] T. Karlsson, P. Persson, U. Skyllberg, C.-M. Mörth, R. Giesler, Characterization of Iron(III) in Organic Soils Using Extended X-ray Absorption Fine Structure Spectroscopy, Environ. Sci. Technol. 42 (2008) 5449–5454, https://doi.org/10.1021/es800322j.

[30] T. Karlsson, P. Persson, Complexes with aquatic organic matter suppress hydrolysis and precipitation of Fe(III), Chem. Geol. 322–323 (2012) 19–27, https://doi.org/10.1016/j.chemgeo.2012.06.003.

[31] T. Karlsson, P. Persson, Coordination chemistry and hydrolysis of Fe(III) in a peat humic acid studied by X-ray absorption spectroscopy, Geochim. Cosmochim. Acta 74 (2010) 30–40, https://doi.org/10.1016/j.gca.2009.09.023.

[32] M. Kleber, K. Eusterhues, M. Keiluweit, C. Mikutta, R. Mikutta, P.S. Nico, in: Chapter One - Mineral-Organic Associations: Formation, Properties, and Relevance in Soil Environments, Academic Press, 2015, pp. 1–140, https://doi.org/10.1016/bs.agron.2014.10.005.

[33] M. Grybos, M. Davranche, G. Gruau, P. Petitjean, Is trace metal release in wetland soils controlled by organic matter mobility or Fe-oxyhydroxides reduction? J. Colloid Interface Sci. 314 (2007) 490–501.

[34] R. Marsac, M. Davranche, G. Gruau, A. Dia, M. Pédrot, M. Le Coz-Bouhnik, N. Briant, Effects of Fe competition on REE binding to humic acid: Origin of REE pattern variability in organic waters, Chem. Geol. 342 (2013) 119–127, https://doi.org/10.1016/j.chemgeo.2013.01.020.

[35] M.J. La Force, S. Fendorf, Solid-phase iron characterization during common selective sequential extractions, Soil Sci. Soc. Am. J. 64 (2000) 1608.

[36] A. Beauvois, D. Vantelon, J. Jestin, M. Bouhnik-Le Coz, C. Catrouillet, V. Briois, T. Bizien, M. Davranche, How crucial is the impact of calcium on the reactivity of iron-organic matter aggregates? Insights from arsenic, J. Hazard. Mater. 404 (2021), 124127, https://doi.org/10.1016/j.jhazmat.2020.124127.

[37] A. Beauvois, D. Vantelon, J. Jestin, A. Dupont, V. Briois, E. Paineau, T. Bizien, A. Pradel, M. Davranche, Aluminum-induced colloidal destabilization of iron-organic matter nanoaggregates, Geochim. Cosmochim. Acta 344 (2023) 1–11, https://doi.org/10.1016/j.gca.2023.01.005.

[38] A. Dia, G. Gruau, G. Olivié-Lauquet, C. Riou, J. Molénat, P. Curmi, The distribution of rare earth elements in groundwaters: assessing the role of source-rock composition, redox changes and colloidal particles, Geochim. Cosmochim. Acta 64 (2000) 4131–4151, https://doi.org/10.1016/S0016-7037(00)00494-4.

[39] O. Pourret, G. Gruau, A. Dia, M. Davranche, J. Molénat, Colloidal Control on the Distribution of Rare Earth Elements in Shallow Groundwaters, Aquat. Geochem. 16 (2010) 31–59, https://doi.org/10.1007/s10498-009-9069-0.

[40] C. Catrouillet, H. Guenet, A.-C. Pierson-Wickmann, A. Dia, M.B. LeCoz, S. Deville, Q. Lenne, Y. Suko, M. Davranche, Rare earth elements as tracers of active colloidal organic matter composition, Environ. Chem. 17 (2020) 133–139.

[41] M. Bau, Scavenging of dissolved yttrium and rare earths by precipitating iron oxyhydroxide: experimental evidence for Ce oxidation, Y-Ho fractionation, and lanthanide tetrad effect, Geochim. Cosmochim. Acta 63 (1999) 67–77, https://doi.org/10.1016/S0016-7037(99)00014-9.

[42] Y. Takahashi, H. Sakami, M. Nomura, Determination of the oxidation state of cerium in rocks by Ce LIII-edge X-ray absorption near-edge structure spectroscopy, Anal. Chim. Acta 468 (2002) 345–354, https://doi.org/10.1016/S0003-2670(02)00709-2.

[43] A.-M. Flank, G. Cauchon, P. Lagarde, S. Bac, M. Janousch, R. Wetter, J.-M. Dubuisson, M. Idir, F. Langlois, T. Moreno, Lucia, a microfocus soft XAS beamline, Nucl. Instrum. Methods Phys. Res. Sect. B Beam Interact. Mater. At. 246 (2006) 269–274.

[44] D. Vantelon, N. Trcera, D. Roy, T. Moreno, D. Mailly, S. Guilet, E. Metchalkov, F. Delmotte, B. Lassalle, P. Lagarde, The LUCIA beamline at SOLEIL, J. Synchrotron Radiat. 23 (2016) 635–640.

[45] B. Ravel, M. Newville, ATHENA, ARTEMIS, HEPHAESTUS: data analysis for X-ray absorption spectroscopy using IFEFFIT, J. Synchrotron Radiat. 12 (2005) 537–541.

[46] C. Hennig, A. Ikeda-Ohno, W. Kraus, S. Weiss, P. Pattison, H. Emerich, P. M. Abdala, A.C. Scheinost, Crystal structure and solution species of Ce (III) and Ce (IV) formates: From mononuclear to hexanuclear complexes, Inorg. Chem. 52 (2013) 11734–11743.

[47] M. Davranche, O. Pourret, G. Gruau, A. Dia, M. Le Coz-Bouhnik, Adsorption of REE (III)-humate complexes onto MnO2: Experimental evidence for cerium anomaly and lanthanide tetrad effect suppression, Geochim. Cosmochim. Acta 69 (2005) 4825–4835, https://doi.org/10.1016/j.gca.2005.06.005.

[48] R. Marsac, M. Davranche, G. Gruau, A. Dia, Metal loading effect on rare earth element binding to humic acid: Experimental and modelling evidence, Geochim. Cosmochim. Acta 74 (2010) 1749–1761, https://doi.org/10.1016/j.gca.2009.12.006.
[49] O. Pourret, M. Davranche, G. Gruau, A. Dia, Rare earth elements complexation with humic acid, Chem. Geol. 243 (2007) 128–141, https://doi.org/10.1016/j.chemgeo.2007.05.018.
[50] K.A. Quinn, R.H. Byrne, J. Schijf, Sorption of yttrium and rare earth elements by amorphous ferric hydroxide: Influence of solution complexation with carbonate, Geochim. Cosmochim. Acta 70 (2006) 4151–4165, https://doi.org/10.1016/j.gca.2006.06.014.
[51] G. Gruau, A. Dia, G. Olivié-Lauquet, M. Davranche, G. Pinay, Controls on the distribution of rare earth elements in shallow groundwaters, Water Res. 38 (2004) 3576–3586, https://doi.org/10.1016/j.watres.2004.04.056.
[52] O.S. Pokrovsky, R.M. Manasypov, S.V. Loiko, L.S. Shirokova, Organic and organo-mineral colloids in discontinuous permafrost zone, Geochim. Cosmochim. Acta 188 (2016) 1–20.
[53] E. Chang, A.W. Brewer, D.M. Park, Y. Jiao, L.N. Lammers, Surface complexation model of rare earth element adsorption onto bacterial surfaces with lanthanide binding tags, Appl. Geochem. 112 (2020), 104478, https://doi.org/10.1016/j.apgeochem.2019.104478.
[54] R.A. Alvarez-Puebla, J.J. Garrido, Effect of pH on the aggregation of a gray humic acid in colloidal and solid states, Chemosphere 59 (2005) 659–667, https://doi.org/10.1016/j.chemosphere.2004.10.021.
[55] M. Pédrot, A. Dia, M. Davranche, Dynamic structure of humic substances: Rare earth elements as a fingerprint, J. Colloid Interface Sci. 345 (2010) 206–213.
[56] H. Kipton, J. Powell, R.M. Town, Solubility and fractionation of humic acid; effect of pH and ionic medium, Anal. Chim. Acta 267 (1992) 47–54, https://doi.org/10.1016/0003-2670(92)85005-Q.
[57] J.P. Pinheiro, A.M. Mota, J.M.R. d'Oliveira, J.M.G. Martinho, Dynamic properties of humic matter by dynamic light scattering and voltammetry, Anal. Chim. Acta 329 (1996) 15–24, https://doi.org/10.1016/0003-2670(96)00097-9.
[58] N. Kloster, M. Brigante, G. Zanini, M. Avena, Aggregation kinetics of humic acids in the presence of calcium ions, Colloids Surf. Physicochem. Eng. Asp. 427 (2013) 76–82, https://doi.org/10.1016/j.colsurfa.2013.03.030.
[59] A.E. Martell, R.M. Smith, Carboxylic Acids, in: Org. Ligands, Springer US, Boston, MA, 1977, pp. 1–171. https://doi.org/10.1007/978-1-4757-1568-2_1.
[60] R. Marsac, M. Davranche, G. Gruau, M. Bouhnik-Le Coz, A. Dia, An improved description of the interactions between rare earth elements and humic acids by modeling: PHREEQC-Model VI coupling, Geochim. Cosmochim. Acta 75 (2011) 5625–5637, https://doi.org/10.1016/j.gca.2011.07.009.
[61] J. Tang, K.H. Johannesson, Speciation of rare earth elements in natural terrestrial waters: assessing the role of dissolved organic matter from the modeling approach, Geochim. Cosmochim. Acta 67 (2003) 2321–2339, https://doi.org/10.1016/S0016-7037(02)01413-8.